



SOLAR LIGHT INDUCED PHOTOCATALYTIC DEGRADATION OF MALACHITE GREEN USING BIVO₄ CATALYST

Prafulla Kumar Panda, Debapriya Pradhan* and Suresh Kumar Dash

Department of Chemistry, ITER, Siksha 'O' Anusandhan (Deemed to be University), Bhubaneswar, Odisha
751030, India

Email ID: debapriyapradhan3@gmail.com

ABSTRACT

A visible light active bismuth vanadate (BiVO₄) nanoparticle was created using a simple, low-cost, and energy-efficient co-precipitation method. X-ray diffraction and Fourier-transform infrared spectroscopy were used to investigate the crystal structure, phase, and details of chemical bonds in the prepared BiVO₄. The optical property of the catalyst, as well as a thorough evaluation of its morphology, was measured using ultraviolet-vis diffuse reflectance spectroscopy and FE-SEM analysis. The elemental composition and purity of the catalyst were determined using EDAX analysis. The degradation of MG under solar light radiation was used to scrutinise the photocatalytic efficiency of the catalyst. Within 75 minutes, BiVO₄ demonstrated 95% degradation efficiency. To evaluate the degradation efficiency of the catalyst, various parameters (pH, concentration, dose, and time) are investigated.

Keywords: BiVO₄ NPs, malachite green dye, Photocatalytic degradation, electron/hole recombination, solar light irradiation.

DOI Number: 10.48047/NQ.2022.20.20.NQ109154

NeuroQuantology2022;20(20): 1518-1526

INTRODUCTION

Hygienic water is required for all forms of life to exist. Environmental protection and remediation are the most pressing issues for humans in the twenty-first century, owing to rapid industrial expansion, depleted water resources, uncontrolled ground water development, environmental pollution, and global warming causing abnormal climatic changes¹. Various industrial sectors, including textiles, dyeing, and printing, emit huge volumes of synthetic organic colours as effluent. Traditional water purification procedures, such as adsorption, flocculation-sedimentation, ion exchange, biological treatment, and filtration, have been shown to be inadequate and expensive, potentially resulting in additional contamination²⁻⁶. In this regard, heterogeneous photo catalysis, with its high oxidation power, low operating temperature, and green-chemistry-related procedures, has gotten a lot of attention in recent decades, promising a tantalising path to meeting global challenges related to the environment, energy, and sustainability thanks to abundant sunlight resources⁷.

Various studies have been conducted on semiconductors such as TiO₂, ZnO, and others that lack efficiency due to fast charge recombination, reduced absorption, greater band gap, and very low reusability. Among the various nano materials, transition metal oxide are found to attract considerable attention for photocatalytic degradation due to the high stability under U.V light, low cost, high resistivity towards corrosion & their relative abundances. The major drawback in using these semiconductors is their large band gap (> 3 e.v) electron hole recombination which reduce their photocatalytic efficiency, moreover they absorb around 2% to 3% of sun's spectrum & active in U.V range⁸. An effective photocatalyst requires large surface area, narrow band gap, fast charge carrier transformations & ability to absorb solar light under visible region. BiVO₄ has gained significant attention among the several investigated oxides with activity under visible light irradiation. This oxide has piqued the interest of researchers owing to its potential uses in a variety of technical domains, since it possesses intriguing features such as Ferro elasticity [7], ionic conductivity [8] and

photochromism⁹⁻¹⁰. BiVO₄ is an n-type semiconductor with excellent chemical and photo stability properties.

Furthermore, its flexible optical and electrical features, as well as a band gap of 2.4 eV, make it an attractive choice for solar energy harvesting¹¹. For the fabrication of BiVO₄ photocatalyst, many techniques have been described, including solid-state reaction, sonochemical, organic decomposition, precipitation, hydrothermal, sol-gel, and others¹². Kudo et al.¹³ used an aqueous technique to synthesise highly crystalline monoclinic and tetragonal BiVO₄ by reacting the layered potassium vanadates KV₃O₈ and K₃V₅O₁₄ with Bi(NO₃)₃ for three days at 20 °C. Guo et al.¹⁴ investigated the photocatalytic degradation of methylene blue using a simple surfactant-free BiVO₄ catalyst. Sarkar et al.¹⁵ used a precursor-mediated growth approach to create a spherical-shaped BiVO₄ photocatalyst and examined the photocatalytic degradation of Rhodamine B under visible light irradiation. Dong et al.¹⁶ produced sponge-like BiVO₄ films with polystyrene (PS) as a pore-forming material and F-doped SnO₂ (FTO) glass as a substrate and demonstrated photoelectrocatalytic phenol degradation under visible light irradiation. Deebasree et al.¹⁷ used a sol-gel-assisted ultra sonication approach to create a BiVO₄ photocatalyst and evaluated the decolourization of methylene blue under visible light irradiation. Chen et al.¹⁸ used a microwave hydrothermal technique to create a BiVO₄ photocatalyst and examined the total water-splitting mechanism. In this study, a simple Co-precipitation method was used to synthesise BiVO₄ photocatalyst, which was then used to degrade Malachite green (MG) under solar light. The effects of various experimental parameters on the photo degradation of MG were investigated, including initial dye concentration, pH, amount of catalyst loading, and agitation time.

MATERIALS AND METHODS

Materials

For preparation of BiVO₄Bi(NO₃)₃·5H₂O (Aldrich, 99.99%), NH₄VO₃ (Aldrich, 99.99%), Concentrated

HNO₃ solution and NaOH (Merck 99.99% purity) chemicals were used.

Preparation of BiVO₄

BiVO₄ was synthesised using a simple co-precipitation method. In a 1:1 molar ratio, Bi(NO₃)₃·5H₂O and NH₄VO₃ were dissolved in 1M HNO₃ solution. After observing a reddish yellow colour, a 1M NaOH solution was added drop by drop to raise the pH value to 10 while vigorously stirring. The resulting pale yellow colour solution was centrifuged and washed several times with distilled water. The filtrate was then dried in an oven before being calcined in a muffle furnace at 500 °C degrees Celsius for 3 hours. The yellow-colored sample was then finely powdered and collected.

Sample Characterisation

Powder X-ray diffraction was used to characterise the structure using a PAN analytical Diffractometer with Cu-K radiation (PW 1830, Philips, Japan) and CuK α radiation, equipped with a Vantec high speed detector. The samples' X-ray diffraction data were collected in the 2 θ range of 10-80°. The morphology of the samples was examined using field emission microscope (ZEISS SUPRA 55). A Perkin Elmer Spectrum version 10.4.3 FTIR spectrophotometer was used to determine the bond vibrational frequencies of the components, while a Perkin Elmer Lambda365 spectrophotometer was used to acquire UV-DRS spectra (to investigate the materials' optical properties). Spectrophotometer (Systronics 2202) was used for study of photocatalytic degradation.

Photocatalytic Experiment

The photocatalytic efficiency of BiVO₄ against MG dye was investigated. A stock solution with a concentration of 100 ppm was prepared for photocatalytic degradation. The photocatalyst's efficiency was evaluated by varying parameters such as pH (3,5,7,9,11), concentration (20,40,60,80ppm), catalyst dose (0,20,30,40mg), and irradiation time (15,30,45,60,75min). Before exposing the photocatalyst-enhanced dye solution to sunlight, it was kept in the dark for 30 minutes to achieve adsorption-desorption equilibrium.

RESULTS AND DISCUSSION

Materials Characterisation

XRD Analysis

The phase formation of crystalline solids is identified using X-ray diffraction (XRD) analysis which is shown in Figure.1 depicts the XRD patterns of BiVO₄. The observed diffraction peaks at 2θ values of 18.690, 28.918, 30.54, 34.5, 35.2,

39.8, 42.37, 45.7, 46.5, 46.9, 49.9, 53.2, 55.7, 58.2, 59.0, 63.2, 65.5, 69.7, 74.3, 75.5, and 76.4 correspond to (001), (013), (004), (200), (020), (211), (015), (123), (204), (024), (2 All of the peaks are associated with the monoclinic phase of BiVO₄ (JCPDS No. 83–1699). Using the Debye-Scherrer formula, the average crystallite size of the BiVO₄ NPs was calculated to be 34.8 nm.

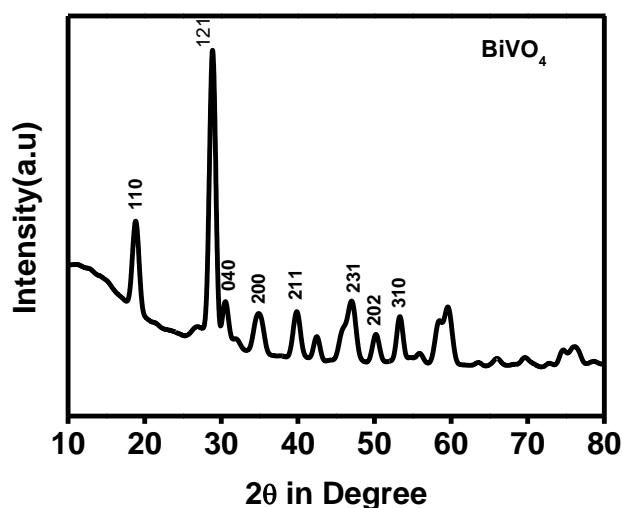


Figure.1. XRD pattern of BiVO₄

All of the diffraction peaks on the product's X-ray diffraction pattern belonged to BiVO₄, implying that the synthesised product was of high purity. The XRD spectrum of the product shows sharp diffraction peaks, indicating that the synthesised BiVO₄ is crystalline.¹⁹

FTIR Analysis

FT-IR spectroscopy is an important analytical technique for determining sample structure and identifying chemical bonds in a molecule. The FT-IR spectrum was captured in the 500-4000 cm⁻¹ wave number range. As shown in Figure.2 the

asymmetric and symmetric stretching bands of the VO₄ unit were attributed to the main absorption bands observed at 725.32 and 830.24 cm⁻¹. The asymmetric stretching and symmetric stretching vibrations of the V-O bond are characterised by the absorption band at 700-900 cm⁻¹. All of the spectra show a weak stretching vibration of the C-O bond derived band at 1383 cm⁻¹ and a bending vibration of absorbed H₂O molecules at 1650 cm⁻¹, which could be due to atmospheric CO₂ absorption during the experiment²⁰.

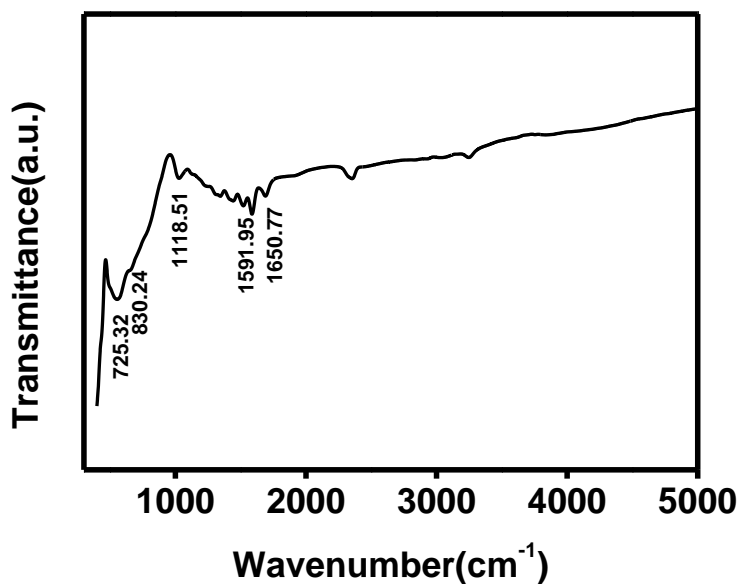


Fig.2 FTIR graph of BiVO₄

Scanning Electron Microscopy (SEM)

Under different magnifications, field emission scanning electron microscopy (FESEM) is used to examine the morphology and elemental composition of BiVO₄ which is shown in Figure.3 .The as-prepared BiVO₄ exemplifies nanoparticle aggregation with a large number of irregular smaller crystals. The EDS analysis of BiVO₄ is shown in Figure.4 that confirmed the presence of Bi, O and V in the NPs. The weight and atomic wt. percentage of Bi, O, V are found to be 67.7, 16.3 and 15.9% and 19.6, 61.6 and 18.8% respectively. The element analytical results agreed well with those previously reported²¹.The absence of other elements proven the purity of BiVO₄ NPs.

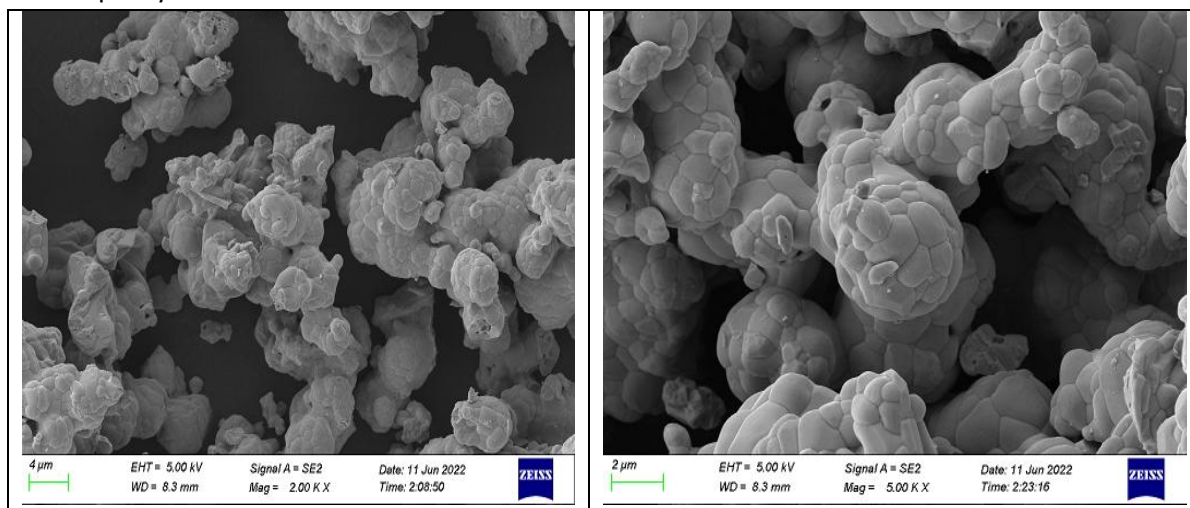


Figure.3 FESEM image of BiVO₄

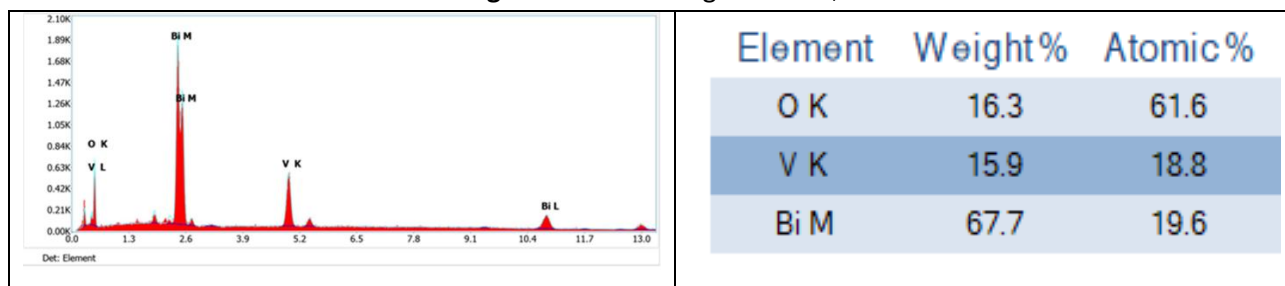


Figure.4. EDS analysis of BiVO₄

UV-DRS Analysis

UV-DRS was used to evaluate the photon absorption abilities of the prepared BiVO₄. The absorption spectrum of BiVO₄ is shown in Figure 5, and the corresponding band gap energy (see Figure 5 inset) was calculated using the equation 1.

$$\alpha h\nu = A (h\nu - E_g)^{1/2} \quad (1)$$

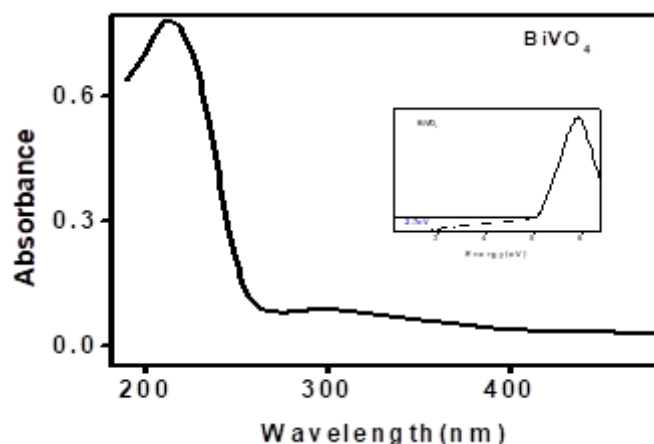


Figure.5. UV-DRS analysis and Band gap energy determination of BiVO₄

where α , ν and h represents the absorption coefficient, frequency of the light and Planck's constant, respectively. The Tauc plot $(\alpha h\nu)^2$ versus photon energy $(h\nu)$ curve can be used to calculate the band gap energy value. BiVO₄ band gap energy was calculated to be 2.6 eV, confirming its potential as a visible light driven photocatalyst. The UV-Vis absorption spectrum of BiVO₄ demonstrates strong optical absorption in the 200-600 nm wavelength range, indicating that BiVO₄ can efficiently absorb visible light and acts as a solar energy driven active photocatalyst for dye degradation. The semiconducting electronic structure is well understood to play an important role in photocatalytic activity²².

Effect of Various parameters on Photocatalytic Degradation

EFFECT OF PH

The effect of pH on the photo degradation efficiency of MG was investigated under solar irradiation at pH 3.0, 5.0, 7.0, 9.0, and 11.0 in the presence of a fixed amount of BiVO₄ (20mg). The natural pH of the MG solution was 7, and BiVO₄ demonstrated photocatalytic degradation efficiency of 65% in 90 minutes. The pH of the MG solution was adjusted using diluted HCL and NaOH solution to investigate the effect of pH on degradation efficiency. Figure 6 depicts the photo catalyst's photo degradation efficiency at various pH levels. As a result, decreasing the pH results in a simultaneous decrease in degradation efficiency, with 11 exhibiting the highest efficiency (88%). The degradation efficiency differed depending on the pH. The less degradation occurs in acidic pH due to electrostatic repulsion because the dye and catalyst surface are both positive. When the pH is raised, there is a strong attraction between the surface of the catalyst and the dye molecule²³⁻²⁴.

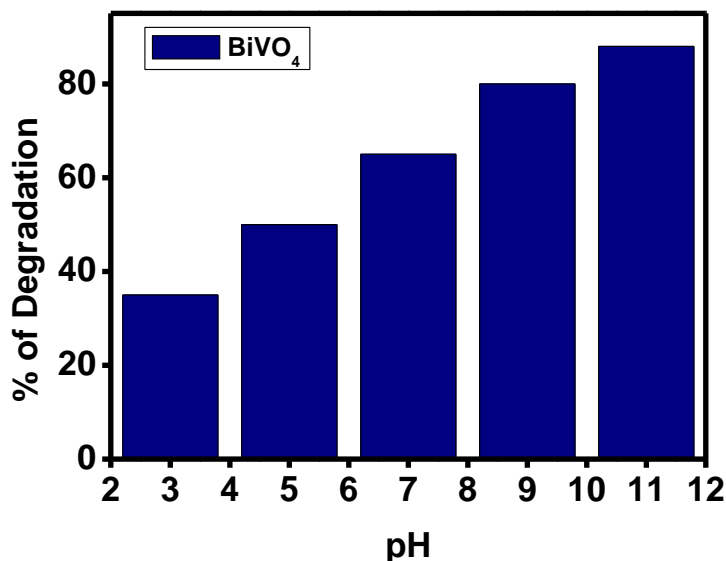


Figure.6. Degradation of MG by BiVO₄ with changing pH values.

Effect of Concentration

The effect of dye concentration (20, 40, 60, 80 ppm) on degradation efficiency was investigated by varying the MG concentration while keeping the catalyst loading and solution pH constant which is shown in figure 7. From figure 7 it is shown that BiVO₄ gave maximum degradation efficiency of 92% on 20 ppm MG solution. The decrease in degradation efficiency with increasing dye concentration is due to an increase in the number of dye molecules, which restrict the incident of light on the catalyst's surface, resulting in the formation of active radical species²⁵.

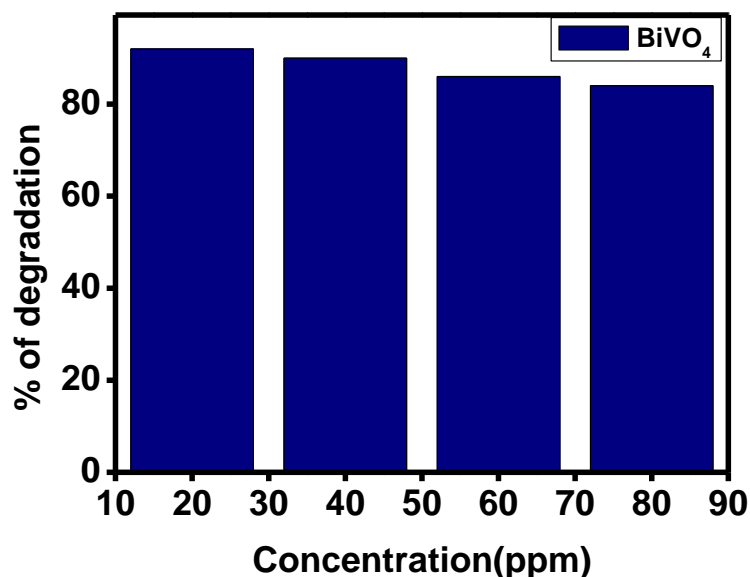


Figure.7. Degradation of MG by BiVO₄ with changing initial concentration

Effect of Catalyst Dose

The impact of the effect of BiVO₄ dose on photo degradation efficiency was examined by varying the amount of catalyst within the range 10-40 mg while keeping pH and concentration constant. From figure 8 it is shown that the maximum degradation of 92% was achieved by 10 mg catalyst dose and there is

decrease in the degradation% with increasing the catalyst dose. However, at a higher catalyst loading there is turbidity in suspensions and light penetration is restricted. The photo degradation rate of MB decreased as a result of the reduced light penetration.

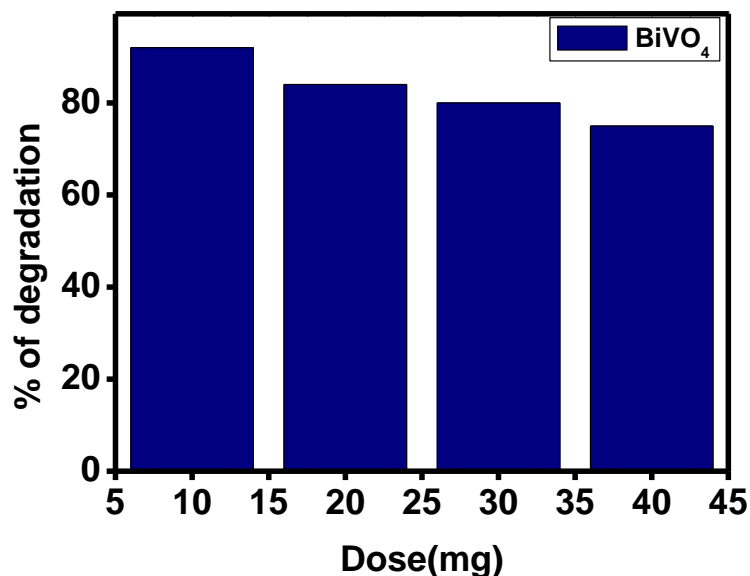


Figure.8. Degradation of MG by BiVO₄ with changing Catalyst dose(mg)

Effect of Time

To investigate the effect of time on the degradation of MG, different ageing times (15,30,45,60,75 min) were used. The degradation percentage increased with time, reaching a peak of 95% at 75 minutes. The degradation vs time and time variant curve is shown in figure 9. Because of the decrease in dye concentration, there is a minimal difference in degradation percentage between times 60 and 75 minutes.

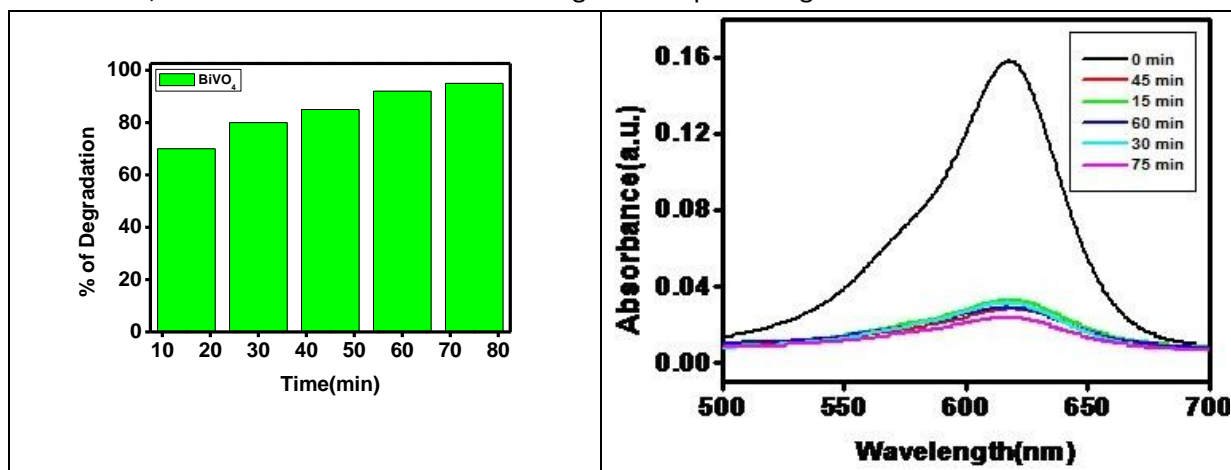


Figure.9. Degradation of MG by BiVO₄ with changing time.

Degradation Mechanism of MG

In a photocatalytic reaction, semiconductor materials absorb photons (light energy) and produce excess electrons (e^-) and holes (h^+) in the conduction band (CB) and valence band (VB), respectively. $\bullet OH$ radicals are formed when the h^+ in the VB reacts with H_2O . Thus, the generated radicals and e^- in the CB are involved in production of superoxide radical which causes the MG degradation, and degradation products are produced (CO_2 , H_2O , etc.)²⁶ as shown in figure 10.

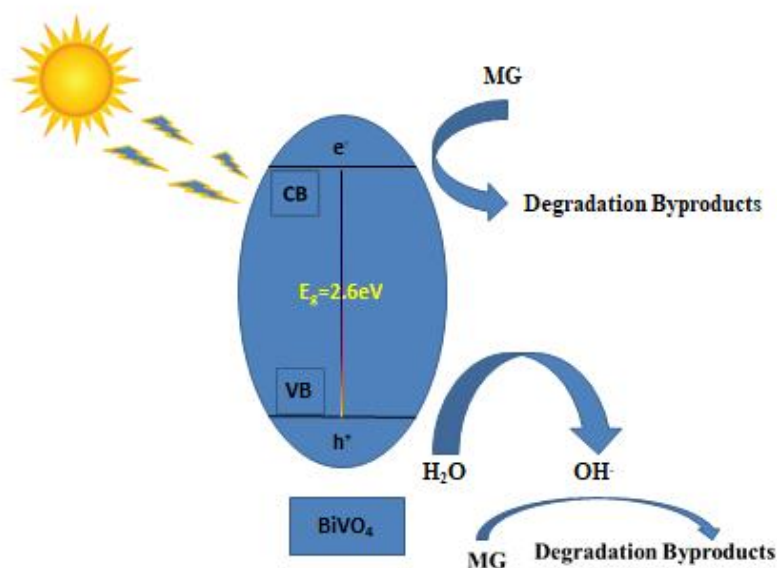


Figure. 10. Possible mechanism for Photocatalytic degradation of MG by BiVO₄.

CONCLUSION

BiVO₄ was developed using the coprecipitation method and characterised using standard techniques (XRD, FTIR, FE-SEM, UV-DRS). The photocatalytic activity of the material was tested by photo degrading Malachite Green in aqueous solution. The material showed a superior capacity to decolorize the dye solution. The photocatalytic efficiency of the photocatalyst was studied by varying parameters like pH, initial concentration, catalyst dose and time. Within 75 minutes, BiVO₄ exhibited 95% photocatalytic degradation towards the MG dye at pH ~11 with 10 mg catalytic dose. The photo-degradation mechanism of MG by BiVO₄ revealed the involvement of hydroxide and superoxide radicals in dye degradation

ACKNOWLEDGMENTS

The authors are grateful to the Department of chemistry, ITER, Siksha 'O' Anusandhan (Deemed To Be University), Bhubaneswar, for providing the help in infra structure, experimental work and in providing chemicals.

REFERENCES

- 1 E. Baldev, D. MubarakAli, A. Ilavarasi, D. Pandiaraj, K. A. S. S. Ishack and N. Thajuddin, *Colloids Surf., B.*, 105, 207–214 (2013).
- 2 N.M. Mubarak, J.N. Sahu, E.C. Abdullah, N.S. Jayakumar, *Sep. Purif. Rev.*, 43, 311–338(2014)
- 3 L. Mohanty, D.S. Pattanayak, R. Singhal, D. Pradhan, S.K. Dash, *Inorg. Chem.Comm.*, 138, 109286(2022)
- 4 D. Pradhan, P.K. Panda, S.K. Dash, *Design Engineering*, 8, 167-174(2021)
- 5 D. Pradhan, P.K. Panda, A. Mishra, E. Falletta, S.K. Dash, *Env. Qual. Mgmt.*, 1-16(2022), Article in Press.
- 6 L. Mohanty, D.S. Pattanayak, S.K. Dash, *J. Indian Chem. Soc.*, 98 (11), 100180(2021).
- 7 Y. Sun, B. Qu, Q. Liu, S. Gao, Z. Yan, W. Yan, B. Pan, S. Wei, Y. Xie, *Nanoscale* 4, 3761–3767(2012).
- 8 I. Khan, K. Saeed and I. Khan, *Arabian J. Chem.*, 12, 908–931 (2019).
- 9 M. Long, W. Cai, J. Cai, B. Zhou, X. Chai, Y. Wu, *J. Phys. Chem. B.*, 110, 20211–20216(2006)
- 10 H. Jiang, H. Endo, H. Natori, M. Nagai, K. Kobayashi, *Mater. Res. Bull.*, 44,700–7006 (2009).
- 11 Y. Hu, J. Fan, C. Pu, H. Li, E. Liu, X. Hu, *J. Photochem. Photobiol. A.*, 337, 172-183(2017).
- 12 Sun, J.X.; Chen, G.; Wu, J.Z.; Dong, H.J.; Xiong, G.H., *Appl. Catal. B Environ.*, 132–133, 304–314 (2013).
- 13 Kudo, A.; Omori, K.; Kato, H., *J. Am. Chem. Soc.*, 121, 11459–11467(1999).

- 14 Guo, M.; He, Q.; Wang, A.; Wang, W.; Fu, Z., *Crystals.*, 6, 81 (2016).
- 15 Sarkar, S.; Chattopadhyay, K.K., *Phys. E.*, 58, 52–58 (2014).
- 16 Dong, L.; Zhang, X.; Dong, X.; Zhang, X.; Ma, C.; Ma, H.; Xue, M.; Shi, F., *J. Colloid Interface Sci.*, 393, 126–129 (2013).
- 17 Deebasree, J.P.; Maheskumar, V.; Vidhya, B., *Ultrason. Sonochem.*, 45, 123–132 (2018).
- 18 Chen, S.H.; Jiang, Y.S.; Lin, H.Y., *ACS Omega.*, 5, 8927–8933 (2020).
- 19 M. Arumugam and M. Y. Choi., *Bull. Korean Chem. Soc.*, 1229-5949 (2020).
- 20 P.Pookmanee, S.Kojinok, R.Puntharod, S.Sangsrichan & S.Phanichphant., *Ferroelectrics.*, 456:1, 45-54 (2013).
- 21 Y. Shen, M. Huang, Y. Huang, J. Alloy. *Compd.*, 496, 287–292 (2010).
- 22 Liu, W., *J. Hazard Mater.*, 181, 1102–1108 (2010).
- 23 V. K. Gupta, R. Jain, A. Mittal, M. Mathur, S. Sikarwar, *J. Colloid Interface Sci.*, 309, 464 (2007).
- 24 A. Franco, M. C. Neves, M. M. Ribeiro Carrott, M. H. Mendon, M. I. Pereira, O. C. Monteiro, *J. Hazard. Mater.*, 161, 545 (2009).
- 25 S. K. Kansal, M. Singh, D. Sud, *J. Hazard. Mater.*, 153, 412 (2008).
- 26 Y. Yan, S. Sun, Y. Song, X. Yan, *Journal of Hazardous Materials.*, 250–251, 106–114 (2013).